On decay constants and orbital distance to the Sun-part III: beta plus and electron capture decay

S. Pomme, S Stroh, J. Paepen, V van Ammel, M. Marouli, A Altzitzoglou, M. Hult, K. Kossert, O. Nähle, S Schrader, et al.

Metrologia

On decay constants and orbital distance to the Sun—part III: beta plus and electron capture decay

OPEN ACCESS
IOP Publishing | Bureau International des Poids et Mesures Metrologia
Metrologia **54** (2017) 36–50 doi:10.1088/1681-7575/54/1/36

On decay constants and orbital distance to the Sun—part III: beta plus and electron capture decay

S Pommé[1], H Stroh[1], J Paepen[1], R Van Ammel[1], M Marouli[1], T Altzitzoglou[1], M Hult[1], K Kossert[2], O Nähle[2], H Schrader[2], F Juget[3], C Bailat[3], Y Nedjadi[3], F Bochud[3], T Buchillier[3], C Michotte[4], S Courte[4], M W van Rooy[5], M J van Staden[5], J Lubbe[5], B R S Simpson[5], A Fazio[6], P De Felice[6], T W Jackson[7], W M Van Wyngaardt[7], M I Reinhard[7], J Golya[7], S Bourke[7], T Roy[8], R Galea[8], J D Keightley[9], K M Ferreira[9], S M Collins[9], A Ceccatelli[10], L Verheyen[11], M Bruggeman[11], B Vodenik[12], M Korun[12], V Chisté[13] and M-N Amiot[13]

[1] European Commission, Joint Research Centre (JRC), Directorate for Nuclear Safety and Security, Retieseweg 111, B-2440 Geel, Belgium
[2] Physikalisch-Technische Bundesanstalt (PTB), Bundesallee 100, 38116 Braunschweig, Germany
[3] Institut de Radiophysique, Lausanne (IRA), Switzerland
[4] Bureau International des Poids et Mesures (BIPM), Pavillon de Breteuil, 92310 Sèvres, France
[5] Radioactivity Standards Laboratory (NMISA), 15 Lower Hope Road, Rosebank 7700, Cape Town, South Africa
[6] National Institute of Ionizing Radiation Metrology (ENEA), Casaccia Research Centre, Via Anguillarese, 301—S.M. Galeria I-00060 Roma, C.P. 2400, I-00100 ROMA A.D., Italy
[7] Australian Nuclear Science and Technology Organisation (ANSTO), Locked Bag 2001, Kirrawee, NSW 2232, Australia
[8] National Research Council of Canada (NRC), 1200 Montreal Road, Ottawa, ON K1A0R6, Canada
[9] National Physical Laboratory (NPL), Hampton Road, Teddington, Middlesex TW11 OLW, UK
[10] Department of Nuclear Sciences and Applications, Terrestrial Environment Laboratory, IAEA Environment Laboratories, International Atomic Energy Agency (IAEA), Vienna International Centre, PO Box 100, 1400 Vienna, Austria
[11] Belgian Nuclear Research Centre (SCK•CEN), Boeretang 200, B-2400 Mol, Belgium
[12] Jožef Stefan Institute (JSI), Jamova 39, 1000 Ljubljana, Slovenia
[13] CEA, LIST, Laboratoire National Henri Becquerel (LNHB), Bât. 602 PC 111, CEA-Saclay, 91191 Gif-sur-Yvette cedex, France

E-mail: stefaan.pomme@ec.europa.eu

Received 22 September 2016, revised 25 October 2016
Accepted for publication 4 November 2016
Published 28 November 2016

Abstract

The hypothesis that seasonal changes in proximity to the Sun cause variation of decay constants at permille level has been tested for radionuclides disintegrating through electron capture and beta plus decay. Activity measurements of ^{22}Na, ^{54}Mn, ^{55}Fe, ^{57}Co, ^{65}Zn, $^{82+85}$Sr, ^{90}Sr, ^{109}Cd, ^{124}Sb, ^{133}Ba, ^{152}Eu, and ^{207}Bi sources were repeated over periods from 200 d up to more than four decades at 14 laboratories across the globe. Residuals from the exponential nuclear decay curves were inspected for annual oscillations. Systematic deviations from a purely exponential decay curve differ from one data set to another and appear attributable to

instabilities in the instrumentation and measurement conditions. Oscillations in phase with Earth's orbital distance to the sun could not be observed within 10^{-4}–10^{-5} range precision. The most stable activity measurements of β^+ and EC decaying sources set an upper limit of 0.006% or less to the amplitude of annual oscillations in the decay rate. There are no apparent indications for systematic oscillations at a level of weeks or months.

Keywords: half-life, decay constant, uncertainty, radioactivity, Sun, neutrino

(Some figures may appear in colour only in the online journal)

1. Introduction

This is part III of a series of three papers investigating annual modulations in measured radioactive decay rates and in particular the claim that decay constants change at permille level in phase with the seasonal variations in Earth–Sun distance. In part I [1], long-term measurements of alpha decay were collected from metrology laboratories across the globe. The decay rates of ^{209}Po, ^{226}Ra, ^{228}Th, ^{230}U, and ^{241}Am sources showed no oscillations in phase with Earth's orbital distance to the sun within 10^{-5}–10^{-6} range precision. The most stable activity measurements of α decaying sources set an upper limit of 0.0006% to 0.006% to the amplitude of annual modulations in the decay rate. In part II [2], evidence was collected and analysed for β^- decaying nuclides. The amplitudes of annual sinusoidal modulations in the most stable measurements were below 0.007% for ^{60}Co, ^{134,137}Cs, ^{90}Sr, and ^{124}Sb and below 0.05% for ^{3}H, ^{14}C, and ^{85}Kr. In part III, the focus is on radionuclides disintegrating through electron capture (EC) and beta plus (β^+) decay.

The rationale behind the project has been discussed in parts I [1] and II [2] and in a summary paper [3]. The issue is similar as for α and β^- decay. Claims have been made in the literature that there are violations of the exponential decay law in the shape of seasonal modulations of permille level amplitude. Theories have been proposed that predict variability of the decay constants. One of the prevailing ideas is that radioactive decay is stimulated by interaction with neutrinos—either solar neutrinos or relic neutrinos from dark matter—and seasonal changes in neutrino flux reaching Earth would cause non-exponential decay. The metrological community has an interest in investigating this issue, because the exponential decay law and the invariability of the decay constants constitute the cornerstone of the common measurement system for radioactivity and all its applications. The aim is to anticipate the metrological consequences if new insights necessitate a different view on radioactivity.

Whereas the experimental evidence of permille-sized seasonal modulations in radioactive decay has been mostly focussed on β^- decay (see e.g [4–6].), similar cases have been reported involving EC and β^+ decay. O'Keefe *et al* [7] reanalysed ^{22}Na/^{44}Ti decay rate ratio data measured by Norman *et al* [8] and reported a weak annual variation at sub-permille level. Ionisation chamber measurements of ^{152}Eu at PTB have been known to show seasonal effects [5, 10], but PTB metrologists related them to varying laboratory conditions affecting the instrumentation [9, 10]. Jenkins and Fischbach [11] claimed that the decay of ^{54}Mn is influenced by solar flares and Mohsinally *et al* [12] reported correlations with solar storms. Jenkins *et al* [5] included ^{54}Mn in the list of nuclides with permille level annual modulations, whereas this was refuted by Silverman [13] on the basis of a mathematical analysis of half-life measurement data by Van Ammel *et al* [14] at the JRC (see section 3.2). From a metrological point of view, the mere observation of seasonal modulations is insufficient proof of the variability of decay constants as long as instrumental instability cannot be ruled out as a plausible cause of the observed effects [15–17].

In this work, activity measurements of ^{22}Na, ^{54}Mn, ^{55}Fe, ^{57}Co, ^{65}Zn, $^{82+85}$Sr, ^{90}Sr, ^{109}Cd, ^{124}Sb, ^{133}Ba, ^{152}Eu, and ^{207}Bi sources have been repeated over periods of 200 d up to 4 decades by different measurement techniques at different laboratories across the globe. The measurement techniques used in this paper are current measurements in an ionisation chamber (IC) [18], detection of gamma rays in a high-purity germanium spectrometer (HPGe) [19], and counting of x-rays at a defined low solid angle with a gas wire proportional counter (PC) [20].

Exponential decay curves were fitted to the measured decay rates and the residuals were inspected for annual modulations, using the same methodology as in [1–3]. The residuals from the fitted decay curve were binned into 8 d periods of the year and averaged to obtain a reduced set of (maximum) 46 residuals evenly distributed over the calendar year. To the averaged residuals, a sinusoidal shape $A\ \sin(2\pi(t + a)/365)$ was fitted in which A is the amplitude, t is the elapsed number of days since New Year, and a is the phase shift expressed in days. The standard uncertainty on the fitted amplitude was determined as the value which increases the variable $\chi^2/(\chi^2/\upsilon)_0$ by a value of one; the chi square χ^2 was divided by the reduced chi square $(\chi^2/\upsilon)_0$ of the fit to protect against unrealistic uncertainty evaluations, e.g. due to correlations between measurements. A summary table of the sinusoid parameter fit values for most of the data sets has been published in [3].

In this paper, graphs are shown of residuals of integrated count rates or ionisation currents (for convenience all types of signals will be represented by the same symbol I) over the measured period as well as multi-annual averages taken over fixed 8 d periods of the year. The uncertainty bars are indicative only: for the individual data they often refer to a short-range repeatability, and for the annual averaged data (maximum 46 data, covering 8 d periods) they were derived from the spread of the input data and the inverse square root of the number of values in each data group. As a reference measure for the expected solar influence, a functional curve is included representing the annual variation of the inverse

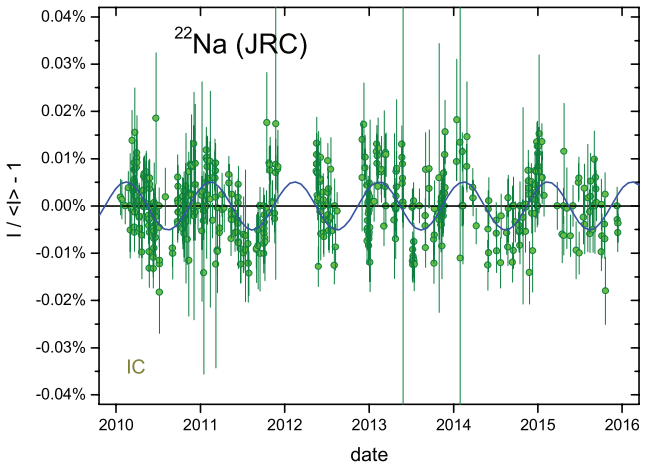

Figure 1. Residuals from exponential decay for ^{22}Na activity measurements with the IG12 ionisation chamber at JRC. The line represents a fitted sinusoidal annual modulation.

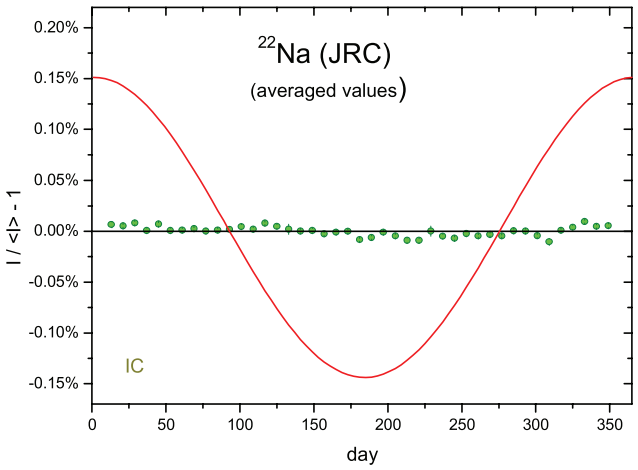

Figure 2. Annual average residuals from exponential decay for ^{22}Na activity measurements with the IG12 IC at JRC. The line represents relative changes in the inverse square of the Earth-Sun distance, normalised to 0.15% amplitude.

square of the Sun–Earth distance, $1/R^2$, renormalized to an amplitude of 0.15% (which is typical for the magnitude of the effect claimed by Jenkins *et al* [5]).

2. Sodium-22

2.1. Decay characteristics

The decay of ^{22}Na (2.6029 (8) a) proceeds through β^+ emission (90.36%) and electron capture (9.64%), both predominantly to the 1275 keV state of ^{22}Ne [21]. The 1275 keV γ-ray and the 511 keV annihilation quanta are easily detectable in an IC or a γ-ray spectrometer. It is an important radionuclide for calibration of γ-ray spectrometers.

According to O'Keefe *et al* [4], there is a weak annual modulation at sub-permille level (0.034%) in the ^{22}Na/^{44}Ti decay rate ratio.

2.2. ^{22}Na @JRC

At the JRC (Geel, Belgium), the decay of a ^{22}Na source in aqueous solution inside a sealed glass vial was followed in the IG12 IC between 2010 and 2016. The fitted half-life is in excellent agreement with the evaluated value in literature [21]. The residuals to an exponential decay curve presented in figure 1 do not exceed 0.02%. Consequently, the presence of permille-level modulations at frequencies of days, weeks, months or even a few years can be excluded. The annual averaged residuals in figure 2 show hints of a very small residual annual oscillation with an amplitude of only $A = 0.0047\ (6)\%$ and a phase of $a = 53$ d. The amplitude and phase are almost identical as for ^{134}Cs measured in the same conditions [2, 3], which points to a common origin of physical or instrumental nature. These results set a new upper limit to the solar effect on ^{22}Na decay—if there is any at all – which is an order of magnitude lower than in [4].

2.3. ^{22}Na @NIST

From 1968 to 1985, a ^{22}Na source was measured 90 times in the NIST ionisation chamber 'A' [22], from which 87 data

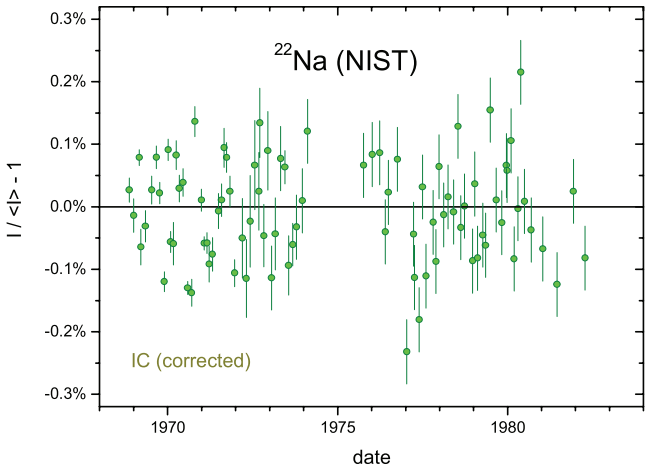

Figure 3. Residuals from exponential decay for ^{22}Na activity measurements with ionisation chamber 'A' at NIST.

were selected for analysis. Linear corrections were applied to the decay rates to compensate for gradual slippage of the source holder as a function of time [23]. The residuals to an exponential decay curve, shown in figure 3, are generally smaller than 0.2% in magnitude, which precludes the presence of permille level modulations with frequencies between a day and a few years. The best fitting sinusoidal modulation to the annual averaged residuals in figure 4 has a negligible amplitude comparable to its standard uncertainty and is out of phase with the JRC data ($A = 0.019\ (12)\%$, $a = 204$ d).

3. Manganese-54

3.1. Decay characteristics

Manganese-54 (312.19 (3) d) decays almost uniquely by electron capture to the 834.855 keV excited level of ^{54}Cr, followed by a gamma transition to the ground state [21]. It is one of the important mono-energetic γ-ray emitters used for calibrations of γ-ray spectrometers.

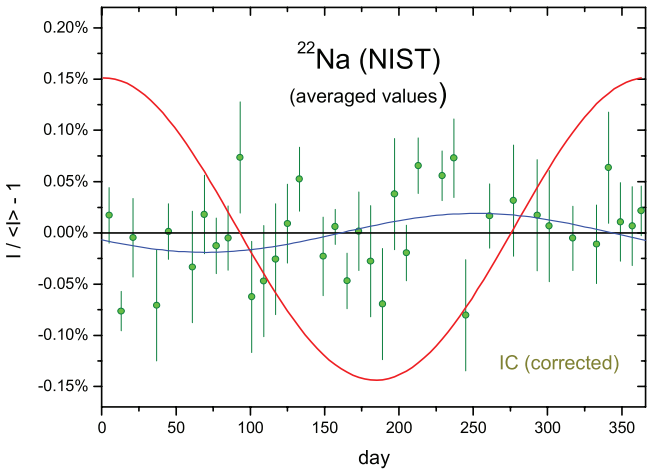

Figure 4. Annual average residuals from exponential decay for ^{22}Na activity measurements with IC 'A' at NIST. The (blue) line with 0.019% amplitude represents a sinusoidal fitted to the data.

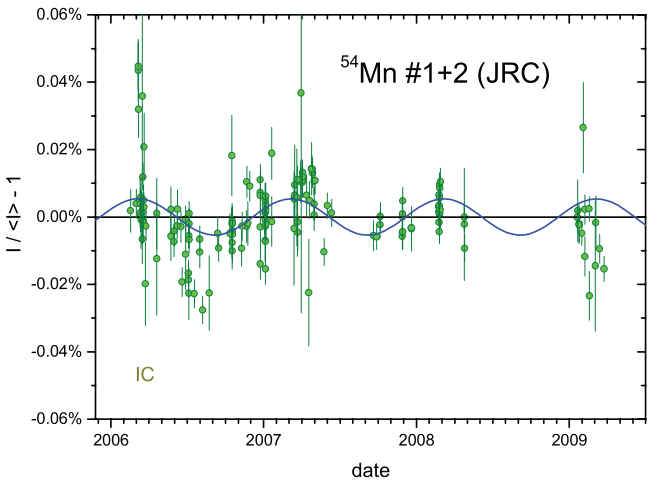

Figure 5. Residuals from exponential decay for ^{54}Mn activity measurements of sources #1 and #2 with the IG12 ionisation chamber at JRC.

There are claims that the decay of ^{54}Mn is influenced by solar neutrinos, visible in seasonal variations of the decay rates [5], and correlations with solar flares [11] and solar storms [12].

3.2. *^{54}Mn @JRC*

Two ^{54}Mn sources in aqueous solution inside a sealed ampoule were measured between 2006 and 2009 in the IG12 IC at the JRC, at initial ionisation currents of 685 pA (#1) and 69 pA (#2) [14]. The data sets of 102 (#1) and 54 (#2) measurements have been combined in one residuals plot (figure 5). The standard deviation is less than 0.01%, which precludes the presence of permille-level modulations at a time scale between a day and a few years. The remaining cyclic instability ($A = 0.005$ (1)% and $a = 28$ d) in the annually averaged residuals in figure 6 has the same low amplitude as the ^{22}Na data in section 2.2. The ^{54}Mn data set of JRC has

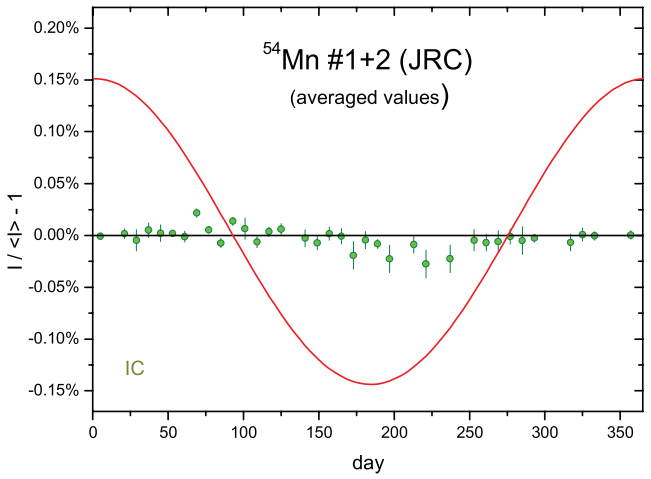

Figure 6. Annual average residuals from exponential decay for ^{54}Mn activity measurements of sources #1 and #2 with the IG12 IC at JRC.

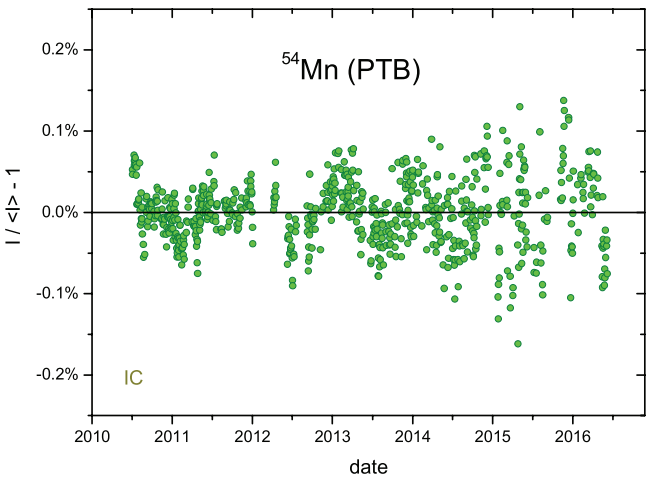

Figure 7. Residuals from exponential decay for ^{54}Mn activity measurements with the IG12/A20 ionisation chamber at PTB.

also been analysed by Silverman [13], who came to similar conclusions.

3.3. *^{54}Mn @PTB*

Between 2010 and 2016, a ^{54}Mn source was measured 724 times in the IG12/A20 IC at the PTB, and 716 data were selected for analysis. Since the data set showed some trending behaviour (<0.25%) over time, it was subdivided in three multi-annual time regions and realigned through a linear transformation in each region. Annual modulations in the residuals remain unaffected by this detrending procedure, while the interfering effects of long-term instabilities are suppressed. The resulting residuals are presented in figure 7 and the annually averaged residuals in figure 8. There is a distinct annual oscillation ($A = 0.014$ (2)%, $a = 78$ d) which has resemblance with effects seen for ^{85}Kr, ^{90}Sr, ^{137}Cs [2], ^{133}Ba (section 9.3), and ^{152}Eu (section 10.5) in the same IC. The effect may be related with the normalisation through a ^{226}Ra check source, which has modulations of the same amplitude

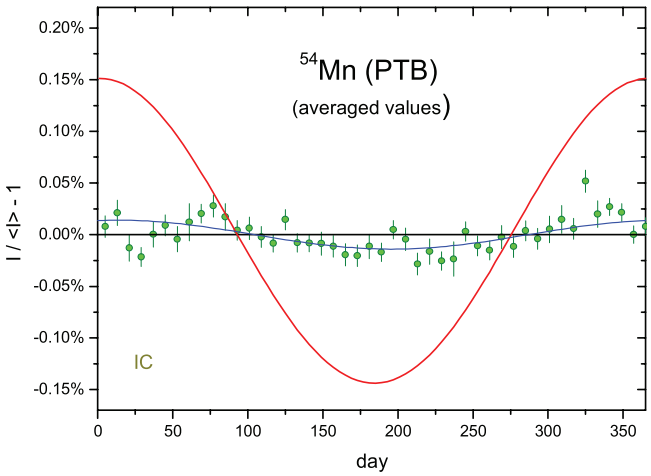

Figure 8. Annual average residuals from exponential decay for ^{54}Mn activity measurements with the IG12/A20 IC at PTB.

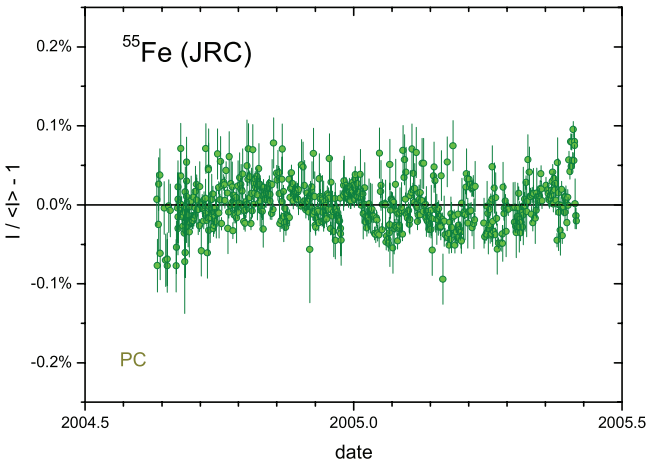

Figure 9. Residuals from exponential decay for ^{55}Fe decay rate measurements with a proportional counter at fixed low solid angle at JRC.

but different phase ($A = 0.016$ (1)%, $a = 194$ d) [1, 3]. The modulations were a factor of 2 smaller in residuals of ^{152}Eu (section 10.5) and ^{154}Eu [2] data that were not normalised to a check source.

4. Iron-55

4.1. Decay characteristics

Iron-55 (2.75 (1) a) decays by EC almost uniquely to the ground state of ^{55}Mn; therefore it produces practically no gamma emission [21]. It can be detected through the x-rays and Auger electrons emitted in the course of atomic rearrangements. The main x-ray has an energy of 5.9 keV, which can be difficult to separate well from interfering signals and to measure in stable conditions.

4.2. ^{55}Fe @JRC

From August 2004 to May 2005 at the JRC, Van Ammel *et al* [24] measured the decay rate of an electrodeposited ^{55}Fe source on a copper backing and covered with an aluminium foil in a fixed defined low solid angle counter [20] with beryllium window and argon(90%)-methane(10%) filled wire proportional counter (PC). The residuals in figure 9 are small but show autocorrelations which complicate the uncertainty assessment of the half-life measurement [15, 24]. Some of these autocorrelations reappear in the annual averages in figure 10 (since the experiment covered less than one year) but in spite of the metrological difficulties it has been demonstrated that physically induced annual cycles, if they occur, must be extremely small ($A = 0.004$ (3)%, $a = 187$ d).

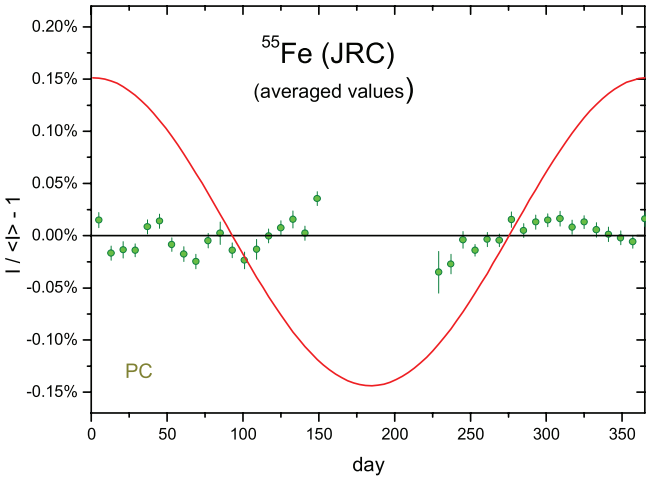

Figure 10. Annual average residuals from exponential decay ^{55}Fe decay rate measurements with a proportional counter at fixed low solid angle at JRC.

5. Cobalt-57

5.1. Decay characteristics

Cobalt-57 (271.80 (5) d) decays by 100% EC to the excited levels of 136.47 keV (99.82%) and 706.42 keV (0.18%) in ^{57}Fe [21]. Some characteristic energies of γ-rays emitted in the decay are 14 keV, 122 keV and 136 keV, which are very useful for efficiency calibration of γ-ray spectrometers at the low-energy side.

5.2. ^{57}Co @NIST

From 1962 to 1966, a ^{57}Co source was measured 99 times in the NIST IC 'A' [22], from which 2 data were excluded from analysis. The residuals to an exponential decay curve, shown in figure 11, are generally smaller than 0.2% in magnitude. The fitted sinusoidal function to the annual averaged residuals in figure 12 is well below permille level ($A = 0.055$ (22)%, $a = 187$ d).

6. Zinc-65

6.1. Decay characteristics

Zinc-65 (244.01 (9) d) decays by EC (50.2%) to the 1115 keV excited level and by EC (48.4%) and β^+ emission (1.4%) to the

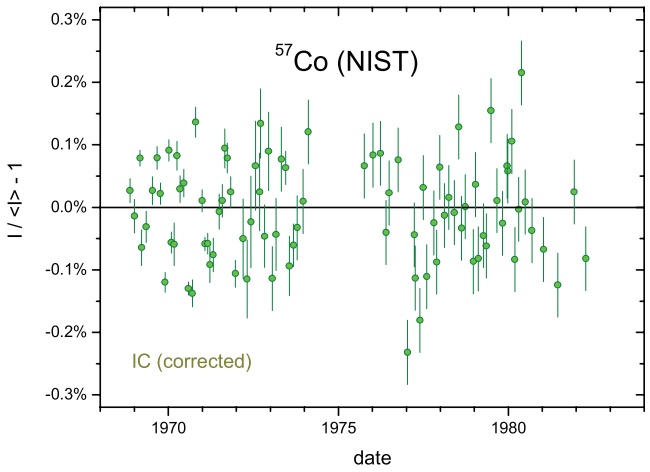

Figure 11. Residuals from exponential decay for ^{57}Co activity measurements with ionisation chamber 'A' at NIST.

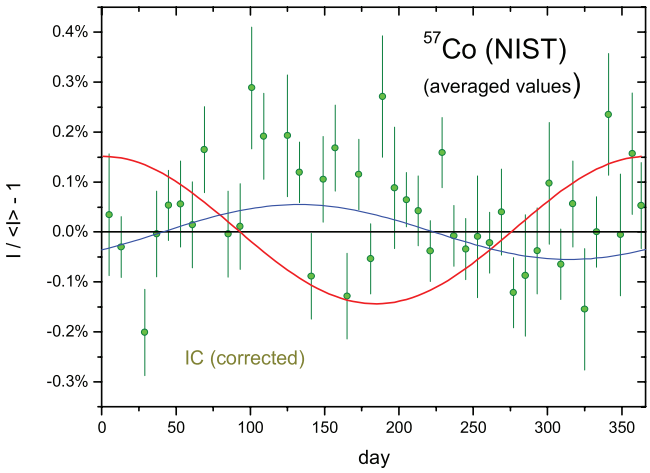

Figure 12. Annual average residuals from exponential decay for ^{57}Co activity measurements with IC 'A' at NIST.

ground state of ^{65}Cu (stable) [21]. It is one of the interesting 'mono-energetic' γ-ray emitters used for detector calibration.

6.2. ^{65}Zn @JRC

The decay of a ^{65}Zn source in aqueous solution was measured by Van Ammel *et al* [25] in the IG12 and ISOCAL III ICs of the JRC between March 2002 and May 2003, in the frame of a half-life determination. The IG12 (20th Century Electronics, UK) ionisation chamber is a well-type ionisation chamber filled with argon to 2 MPa pressure, shielded with 5-cm-thick lead bricks and connected to a current integrating electrometer which incorporates an external feedback air-spaced capacitor. When the output voltage reaches a lower or upper discriminator level, a precision digital voltmeter is sampled. The ISOCAL III ionisation chamber has no shielding, and the resulting current is measured directly with a Keithley 617 electrometer. Each measurement consisted of typically 3000 samples of the current, at regular time intervals of 1 s. Outliers were removed and one average value was

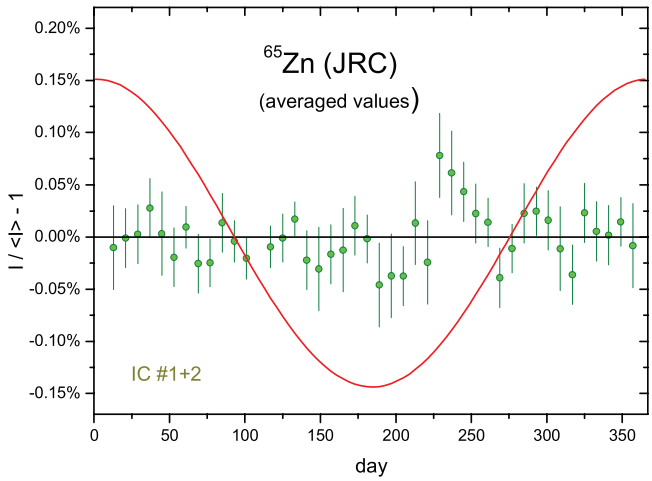

Figure 13. Annual average residuals from exponential decay for ^{65}Zn activity measurements with the IG12 and ISOCAL III ionisation chambers at JRC.

taken per measurement. In total, 140 data points from both ICs were combined and annually averaged data are presented in figure 13. The annual oscillations do not rise above the 10^{-5} level ($A = 0.008\ (4)\%$, $a = 163$ d).

7. Strontium-82 + 85

7.1. Decay characteristics

Strontium-82 (25.347 (17) d) decays by EC to the ground state of ^{82}Rb (1.2652 (45) min), which decays by β^+ emission and EC to ^{82}Kr. Strontium-85 (64.850 (7) d) decays by EC to stable ^{85}Rb, mainly through the excited state at 514 keV [21].

7.2. ^{82,85}Sr @NIST

In 2007–2008 at the NIST, the activity of a ^{82}Sr/^{82}Rb + ^{85}Sr source (Ampoule No. 1951) was measured for 200 d [26] with the ionisation chamber 'AUTOIC' [27], which is different than IC 'A' used for most half-life measurements in the last half century [22]. Whereas the daughter nuclide ^{82}Rb was in equilibrium with the ^{82}Sr, the ^{85}Sr contribution—mainly significant towards the end of the experiment—required the fit of an additional exponential function to the decay curve, the ^{85}Sr half-life parameter being fixed at the literature value. The ratio of the AUTOIC responses to the ^{82}Sr/^{85}Sr components was 2.5 at the reference time.

Additional activity measurements (Source No.1952) were performed by γ-ray spectrometry using a HPGe detector. The ratio of the net gamma-ray emission rates of the 776.517 keV ^{82}Sr γ-ray line to the 661.657 keV ^{137}Cs γ-ray line was followed for 222 d. The residuals to the fit of the decay curves have been published by Pibida *et al* [26]. The HPGe data are quite stable ($A = 0.073\ (75)\%$, $a = 163$ d), but the IC measurements even more so with a fitted amplitude for annual modulations in the 10^{-6} level ($A = 0.0006\ (27)\%$, $a = 240$ d). The annual averaged residuals of the IC measurements are shown in figure 14.

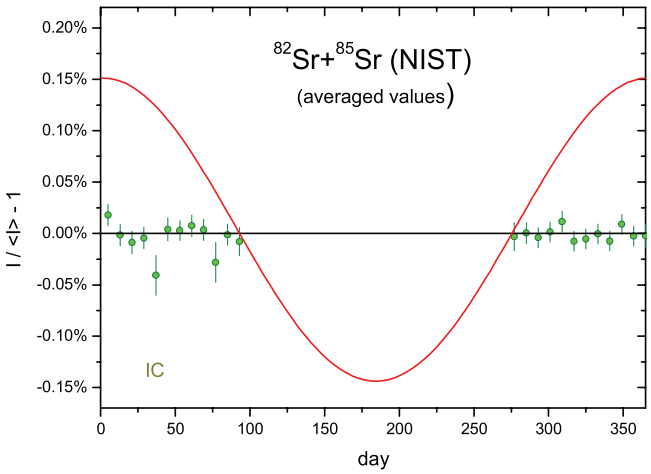

Figure 14. Annual average residuals from exponential decay for ^{82}Sr and ^{85}Sr activity measurements with ionisation chamber 'AUTOIC' at NIST.

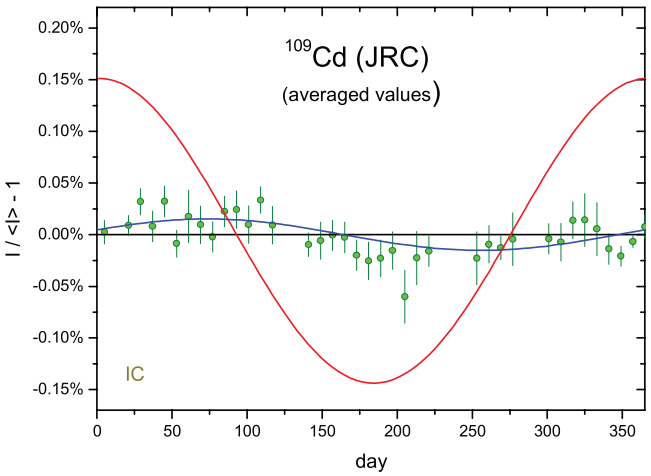

Figure 16. Annual average residuals from exponential decay for ^{109}Cd activity measurements with the IG12 IC at JRC. The (blue) line with 0.015% amplitude represents a sinusoidal fitted to the data.

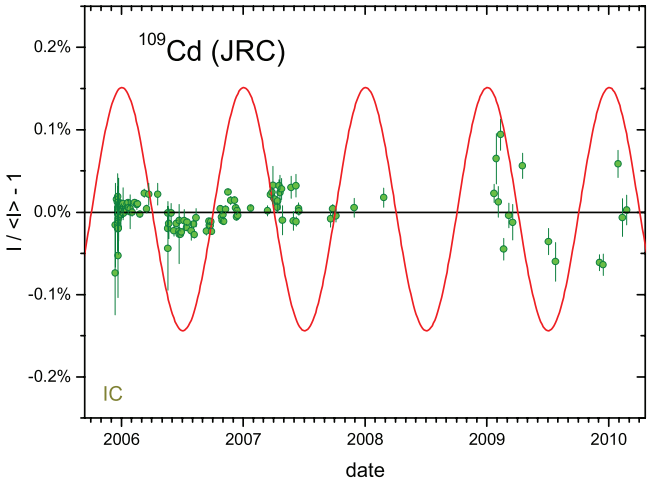

Figure 15. Residuals from exponential decay for ^{109}Cd activity measurements with the IG12 IC at JRC. The line represents relative changes in the inverse square of the Earth–Sun distance, normalised to 0.15% amplitude.

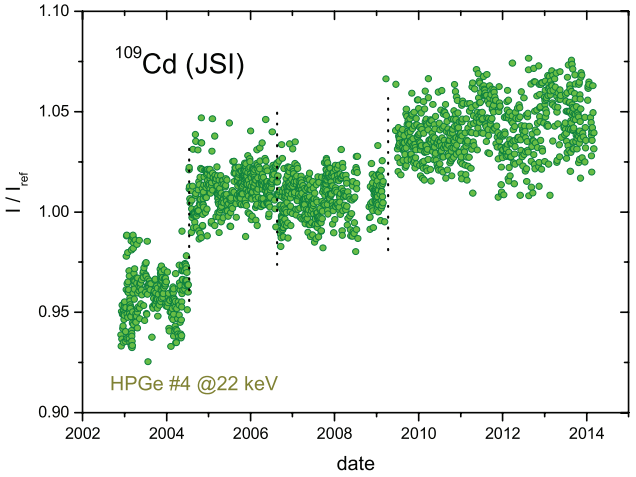

Figure 17. Residuals from exponential decay for ^{109}Cd decay rate measurements by γ-ray spectrometry of the 22 keV transition with HPGe #4 at JSI. The jumps correspond to recalibrations of the detector.

8. Cadmium-109

8.1. Decay characteristics

Cadmium-109 (462.29 (30) d) decays by EC to the isomeric state of ^{109}Ag, followed by emission of an 88 keV γ-ray [21]. This nuclide is often used for efficiency calibrations of γ-ray spectrometers in the low-energy region.

8.2. ^{109}Cd @JRC

At the JRC between 2006 and 2010, measurements with the IG12 IC of a ^{109}Cd source in aqueous solution inside a glass ampoule were used for an accurate half-life determination [28]. In parallel, an additional series of measurements was performed by γ-ray spectrometry, relative to an ^{241}Am reference source. The spectrometry residuals were within 0.1%–0.3% and the IC data (figure 15) within 0.03%–0.08%, which is less precise than for other nuclides due to the lower initial source activity and IC current (11.7 pA). The residual annual instability of the IC data (figure 16) has an amplitude of $A = 0.015\ (4)\%$ and a phase of $a = 18$ d.

8.3. ^{109}Cd @JSI

Besides the 88 keV γ ray, 22 keV x-rays are emitted after the EC decay of ^{109}Cd or as a consequence of internal conversion of ^{109m}Ag ($T_{1/2} = 39.7$ s). Both emissions are regularly measured in HPGe detectors at the JSI (Slovenia). Due to the low energy of the radiation, their detection is very sensitive to absorption effects and small changes in geometry. From 4 data sets measured between 1998 and 2014/2016 (see figures 17–20), 3 were selected and compensated for recalibrations of the detector and systematic drift in the initial part of the 88 keV results in detector #3. The 22 keV data in detector #3 were excluded because of the saw-tooth drift. Thus restricting the analysis

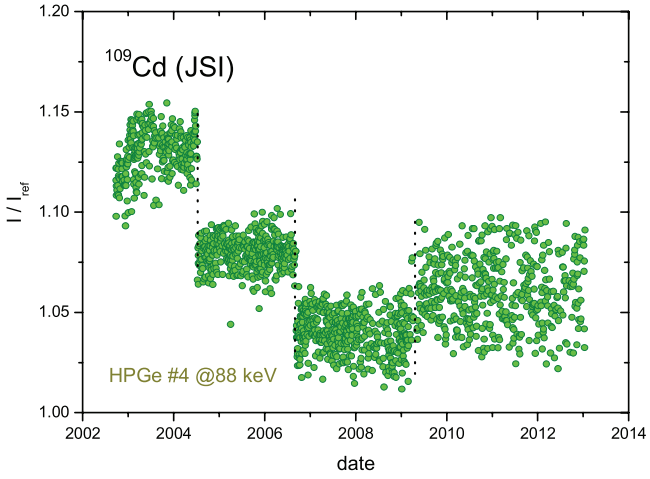

Figure 18. Residuals from exponential decay for ^{109}Cd decay rate measurements by γ-ray spectrometry of the 88 keV transition with HPGe #4 at JSI. The jumps correspond to recalibrations of the detector.

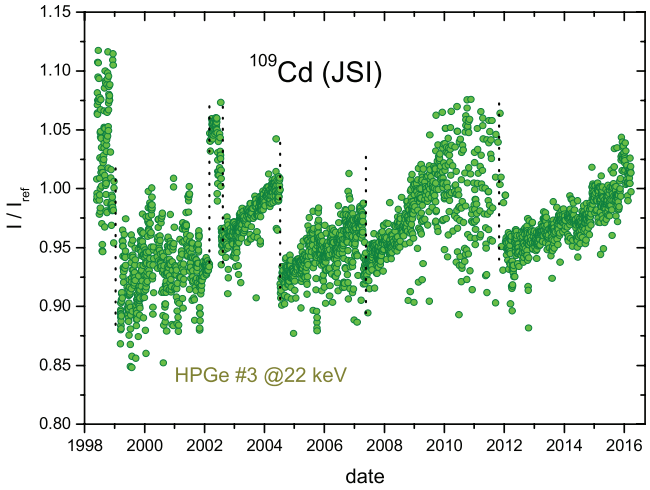

Figure 19. Residuals from exponential decay for ^{109}Cd decay rate measurements by γ-ray spectrometry of the 22 keV transition with HPGe #3 at JSI. The jumps correspond to recalibrations of the detector.

to residuals in the flat regions, one obtains annual averages (figure 21) with a mild seasonal effect ($A = 0.035\ (24)\%$, $a = 346$ d). More importantly, these data sets, in comparison with the ^{60}Co data [2] on the same detectors, demonstrate how detection instability strongly depends on the energy of the radiation.

8.4. ^{109}Cd @NIST

Between 1976 and 1981, the decay of a ^{109}Cd source was measured in the IC 'A' at the NIST [22]. Linear detrending corrections (<0.4%) have been applied over three time zones to suppress the influence of long-term drift on the residuals and to focus the search on systematic annual effects. The residuals to an exponential decay curve, presented in figure 22, are typically a few permille. The annual averages in figure 23 have magnitudes around a permille, but appear to be randomly

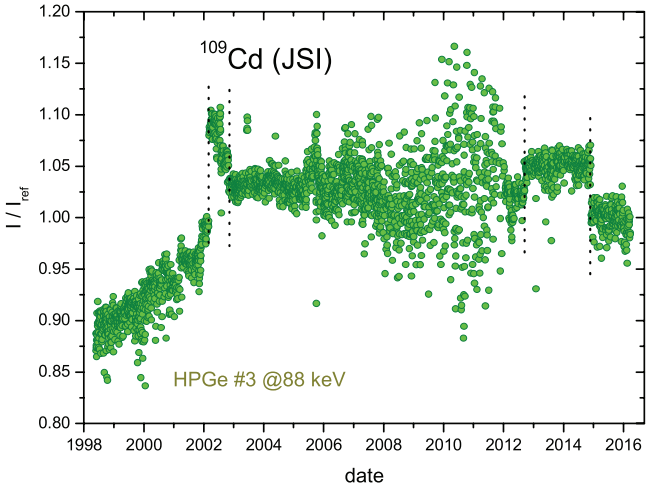

Figure 20. Residuals from exponential decay for ^{109}Cd decay rate measurements by γ-ray spectrometry of the 88 keV transition with HPGe #3 at JSI. The jumps correspond to recalibrations of the detector.

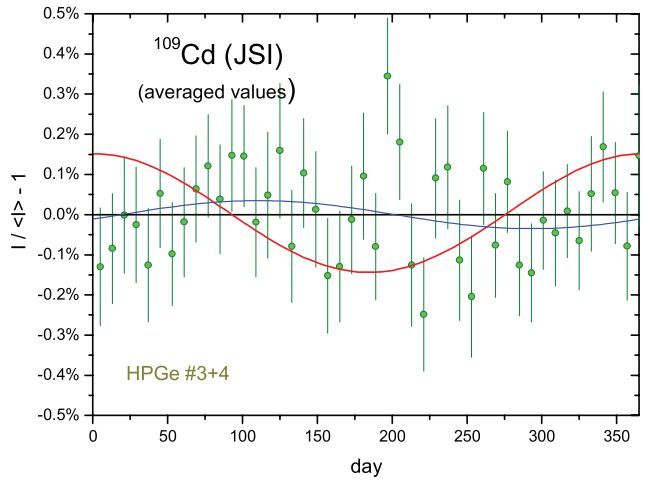

Figure 21. Annual average residuals from exponential decay for selected stable ^{109}Cd decay rate measurement data in figures 17, 18 and 20 obtained at JSI.

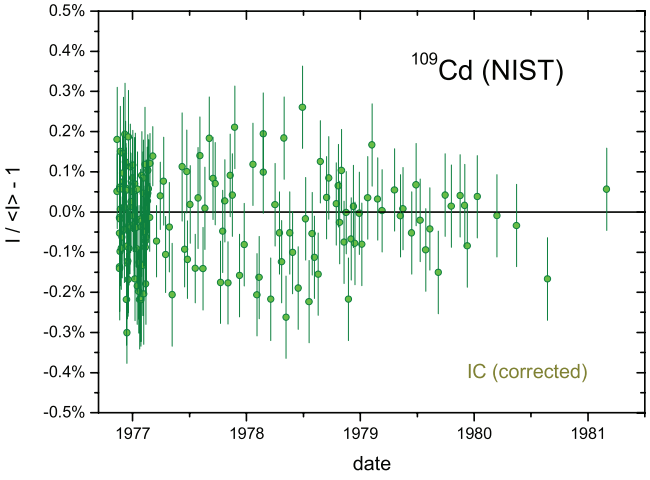

Figure 22. Residuals from exponential decay for ^{109}Cd activity measurements with ionisation chamber 'A' at NIST.

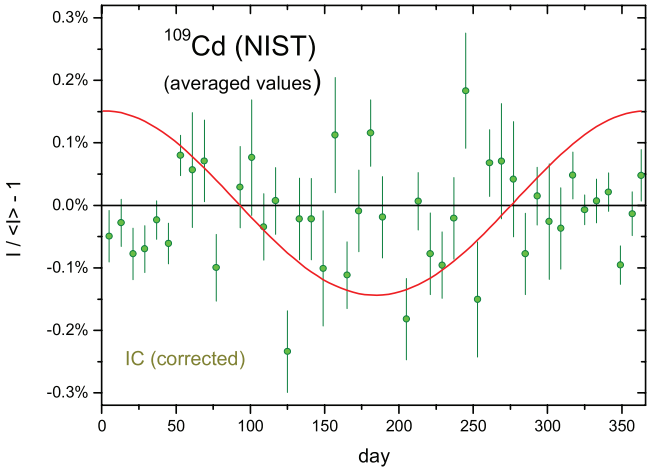

Figure 23. Annual average residuals from exponential decay for ^{109}Cd activity measurements with IC 'A' at NIST.

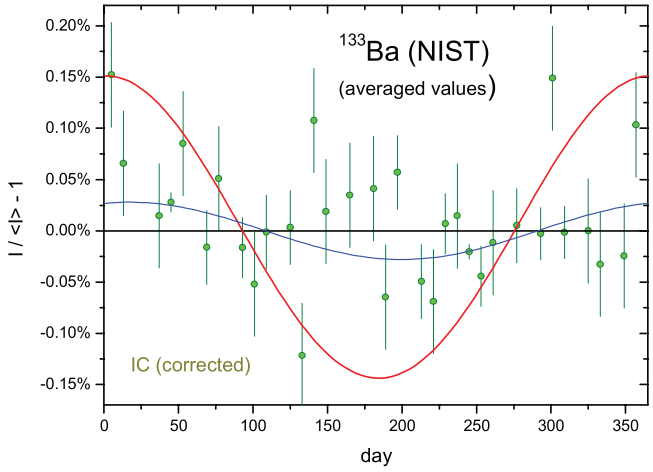

Figure 25. Annual average residuals from exponential decay for ^{133}Ba activity measurements with IC 'A' at NIST.

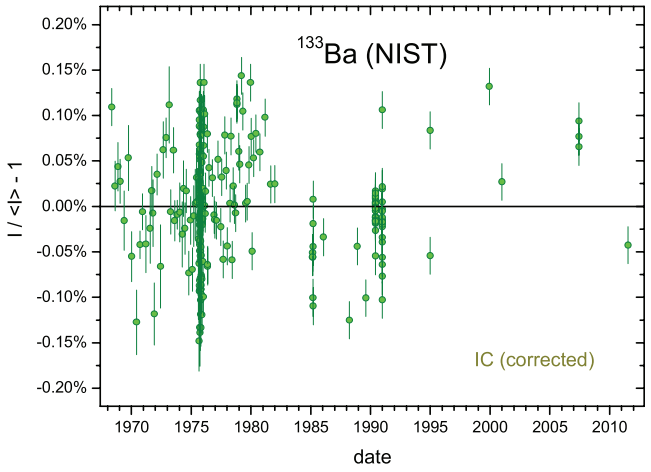

Figure 24. Residuals from exponential decay for ^{133}Ba activity measurements with IC 'A' at NIST.

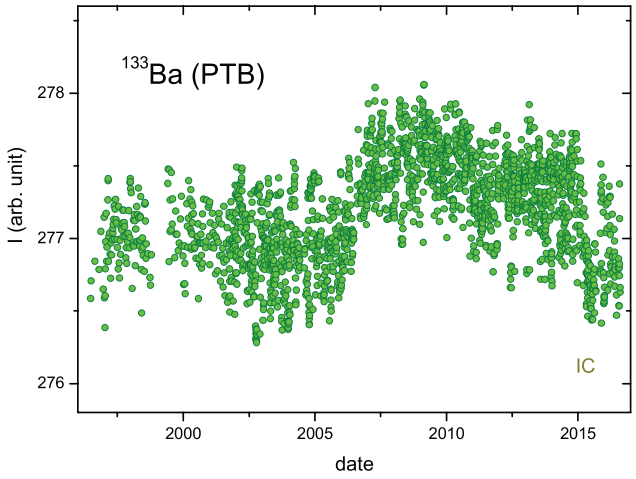

Figure 26. Decay-corrected ionisation currents of a ^{133}Ba source (relative to a ^{226}Ra check source) in the IG12 IC at PTB as a function of date of measurement.

spread and show no significant signs of annual seasonality ($A = 0.013\ (15)\%$, $a = 220$ d).

9. Barium-133

9.1. Decay characteristics

Barium-133 (10.539 (6) a) disintegrates by EC (100%) mainly to two excited levels of ^{133}Cs at 437 keV (85.14%) and 383 keV (14.5%) [21]. It is frequently used for efficiency calibration of γ-ray spectrometers at the low-energy side, owing to characteristic γ emissions of 80.9 keV, 302.8 keV and 356 keV.

According to Jenkins *et al* [5] the decay of ^{133}Ba exhibits 'strong' annual modulations as well as a 2-yearly oscillation tentatively associated with a 'Rieger' *r*-mode oscillation in the solar neutrino flux [29]. It was repeated by Sturrock *et al* [30] that 'these results are compatible with a solar influence' and that 'it is possible that ^{133}Ba measurements are also subject to a non-solar (possibly cosmic) influence'.

9.2. ^{133}Ba @NIST

A ^{133}Ba source was measured 138 times from 1979 to 2012 with the IC 'A' [22] at the NIST. A linear adjustment was made for the time period after 1991 and 7 among the most recent measurements were excluded from the analysis because of a growing bias. In figure 24, the residuals from exponential decay do not exceed a magnitude of 0.15%. Since the data were not evenly distributed, several averaged residuals in figure 25 show a similar precision and a relatively mild seasonal modulation ($A = 0.028\ (8)\%$, $a = 74$ d). The data do not confirm the claim of 'strong' annual modulations [5].

9.3. ^{133}Ba @PTB

From 1996 to 2016, the ionisation current from a ^{133}Ba source was measured 2158 times with an IC at the PTB and the data were analysed relative to the ^{226}Ra check source. The decay-corrected IC output in figure 26 shows a 2-permille-level

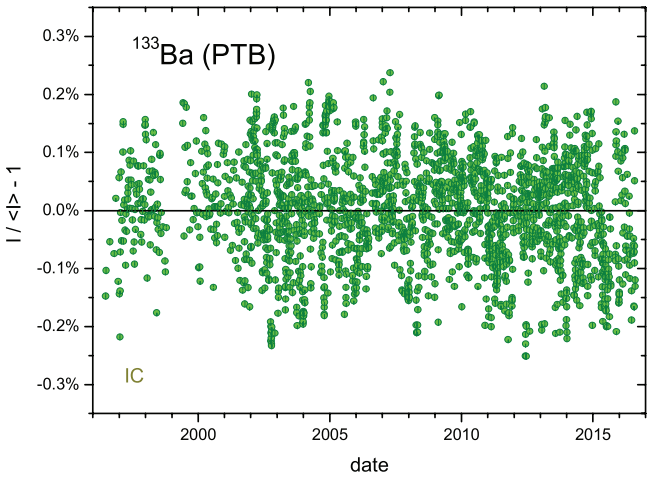

Figure 27. Residuals from exponential decay for ^{133}Ba ionisation current measurements with the IG12 IC at PTB, after applying linear detrending corrections.

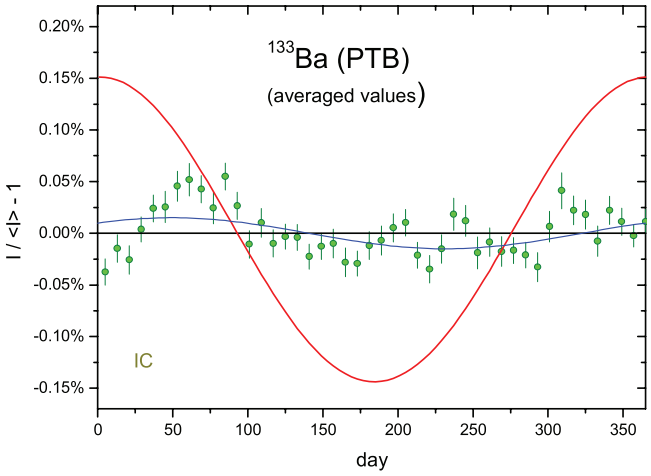

Figure 28. Annual average residuals from exponential decay for ^{133}Ba ionisation current measurements with the IG12 IC at PTB.

long-term drift, very similar to instabilities observed with other nuclides measured over the same period (see e.g. ^{85}Kr [2]). This was compensated for in this work by linear adjustments over 4 time regions and exclusion of 61 extreme data (in value or uncertainty). The resulting residuals in figure 27 have a standard deviation of 0.09% and show some local non-random structures. It is suspected that this particular solution is chemically not stable, which might—at least partly—explain why the residuals are larger than expected considering the rather high ionisation current. The averaged residuals in figure 28 do not adhere smoothly to a sinusoidal function, but nevertheless the fit exhibits an annual modulation of comparable amplitude as for other nuclides in the same IC ($A = 0.015\ (4)\%$, $a = 46$ d).

10. Europium-152

10.1. Decay characteristics

Europium-152 (13.522 (16) a) follows three decay paths: electron capture (72.1%), β^+ emission (0.027%) and β^- emission (27.9%) [21]. It is a typical multi-gamma emitter covering a wide energy range, which makes it convenient for efficiency calibration of HPGe detectors, in spite of true coincidence summing effects in close geometries.

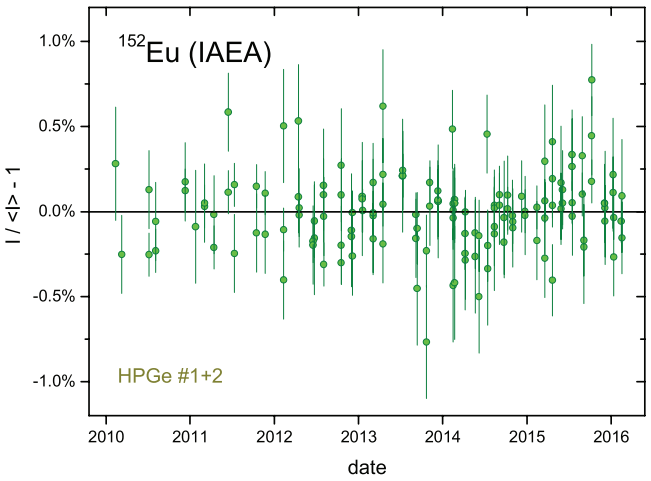

Figure 29. Residuals from exponential decay for ^{152}Eu activity measurements by γ-ray spectrometry with two HPGe detectors at IAEA.

Sturrock *et al* [30] analysed the ^{152}Eu decay rates measured from 1990 to 1995 with the IG12/A20 IC at the PTB and observed annual oscillations in the 0.1% range. They concluded that 'these results are compatible with a solar influence, and do not appear to be compatible with an experimental or environmental influence'. In section 10.5, it will be shown that these oscillations reduced significantly since the replacement of the electrometer in October 1998, which invalidates this interpretation.

10.2. ^{152}Eu @IAEA

At the Terrestrial Environment Laboratory of the IAEA (Seibersdorf, Austria), a ^{152}Eu point source was measured on two HPGe detectors for quality control between 2010 and 2016. Four data sets were derived from the background-corrected count integral of the γ-ray spectra and from the sum of net peak areas of the 40, 122, 344, 778, 964 and 1408 keV emissions. After elimination of extreme data, 143 residuals of typically 0.1%–0.3% were combined in figure 29. The average deviations in figure 30 are free of annual oscillations below permille level ($A = 0.020\ (24)\%$, $a = 162$ d).

10.3. ^{152}Eu @SCK

A wealth of ^{152}Eu γ-ray spectrometry data was collected at the SCK•CEN (Belgium) on 8 HPGe detectors, in parallel with ^{241}Am mixed in the same source [1]. The net peak areas of three transitions at 122 keV, 779 keV and 1408 keV have been followed between 2008 and 2016. The decay-corrected peak areas (see e.g. figure 31) show a quasi-linearly increasing trend—probably caused by uncompensated count loss through pulse pileup—and a jump in 2011 due to a change in data acquisition system [31]. The 24 data sets were linearised and connected by means of the fit of two slopes and a scaling factor. Three groups of results were averaged: two detectors

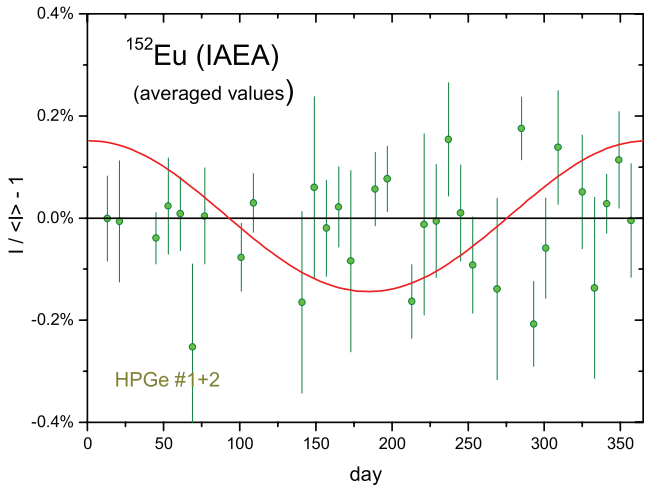

Figure 30. Annual average residuals from exponential decay for ^{152}Eu activity measurements by γ-ray spectrometry with two HPGe detectors at IAEA.

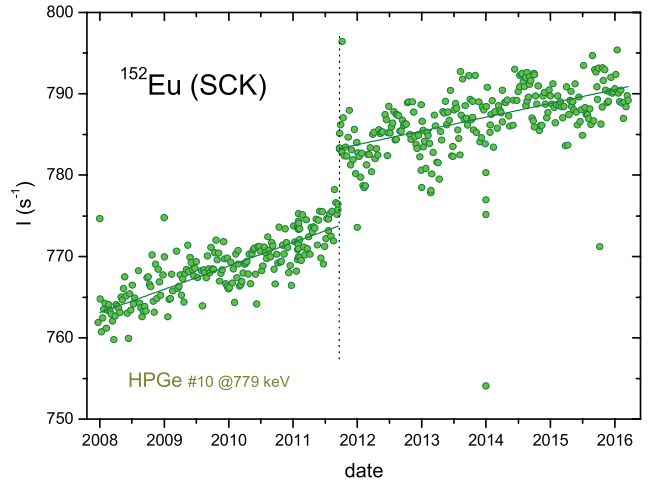

Figure 31. Decay-corrected integrated net peak count rates at 779 keV from the decay of ^{152}Eu measured by γ-ray spectrometry with the HPGe #10 detector at SCK. The jump corresponds to a change in data acquisition system.

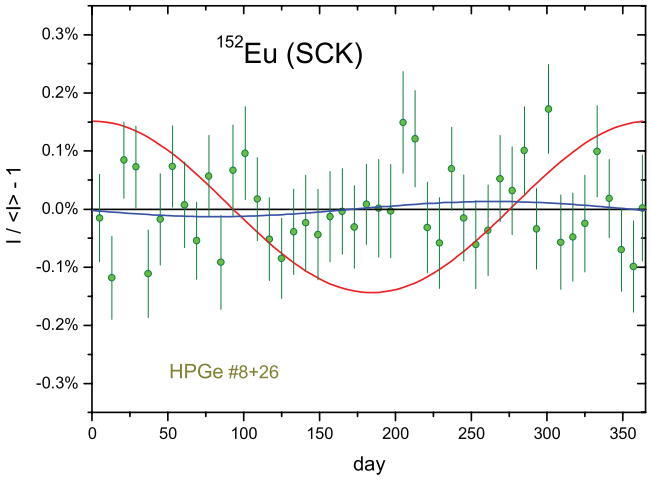

Figure 32. Annual average residuals from exponential decay for ^{152}Eu decay rate measurements by γ-ray spectrometry with HPGe detectors #8 and #26 at SCK. The fitted sinusoidal has an amplitude of 0.013%.

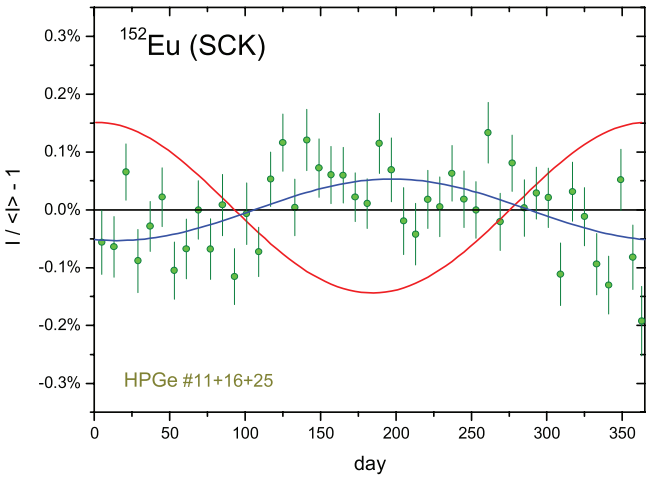

Figure 33. Annual average residuals from exponential decay for ^{152}Eu decay rate measurements by γ-ray spectrometry with HPGe detectors #11, #16 and #25 at SCK. The fitted sinusoidal has an amplitude of 0.053%.

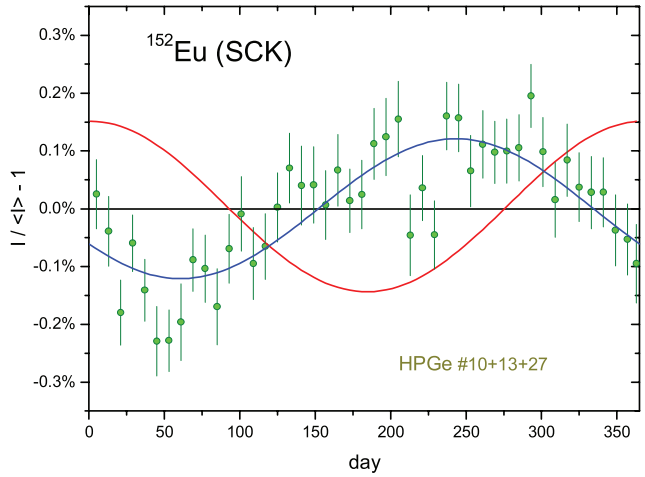

Figure 34. Annual average residuals from exponential decay for ^{152}Eu decay rate measurements by γ-ray spectrometry with HPGe detectors #10, #13 and #27 at SCK. The fitted sinusoidal has an amplitude of 0.121%.

showing no annual effects in figure 32 ($A = 0.013$ (14)%, $a = 192$ d), three detectors with intermediately sized oscillations in figure 33 ($A = 0.053$ (13)%, $a = 259$ d), and three with large oscillations in figure 34 ($A = 0.121$ (13)%, $a = 213$ d). There is clearly no common annual effect in the activity of the ^{152}Eu source, therefore amplitudes above 0.01% cannot be ascribed to variability of the decay constant in correlation with Earth–Sun distance.

Several authors have speculated that beta decay would be susceptible to 'external' influences and alpha decay not, which would explain why less seasonal effects have been observed in alpha decay (see e.g. [5–7, 29, 32]). From a metrological point of view, an explanation could be that it is easier to establish measurement stability for alpha particles with high, discrete energies than for beta particles with lower, variable energies. When not measuring the particles but the subsequent γ-ray emission, the metrological difficulty is similar for both types of decay. It turns out that the annual oscillations of the ^{241}Am (α decay) γ-ray data are almost identical to those of the ^{152}Eu (EC, β^-, β^+ decay) data

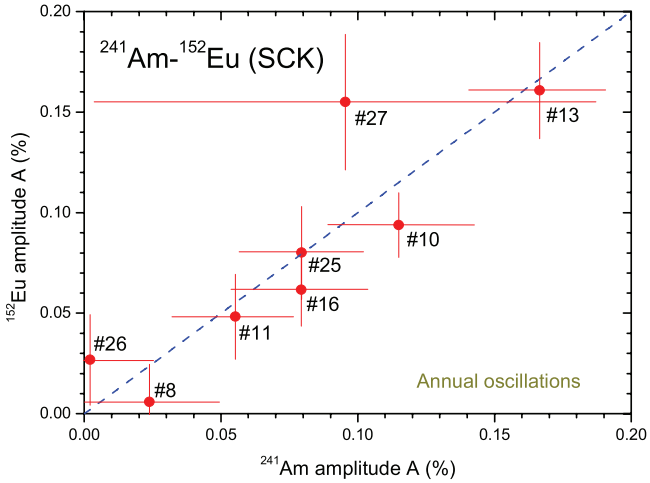

Figure 35. Amplitude of average annual oscillations in the decay rate of ^{241}Am and ^{152}Eu measured by γ-ray spectrometry with 8 HPGe detectors at SCK between 2008 and 2016.

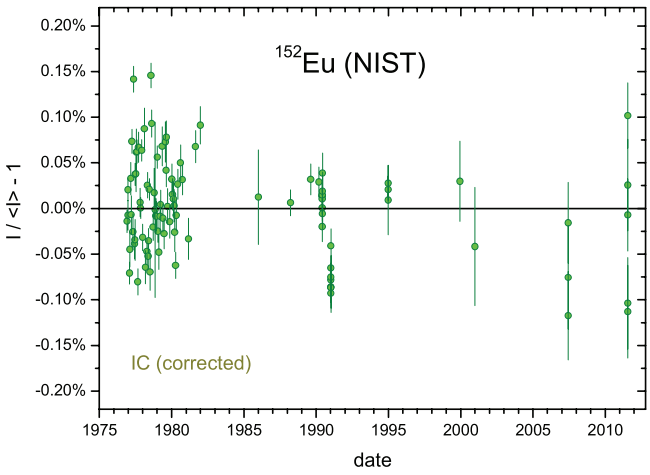

Figure 36. Residuals from exponential decay for ^{152}Eu activity measurements with ionisation chamber 'A' at NIST.

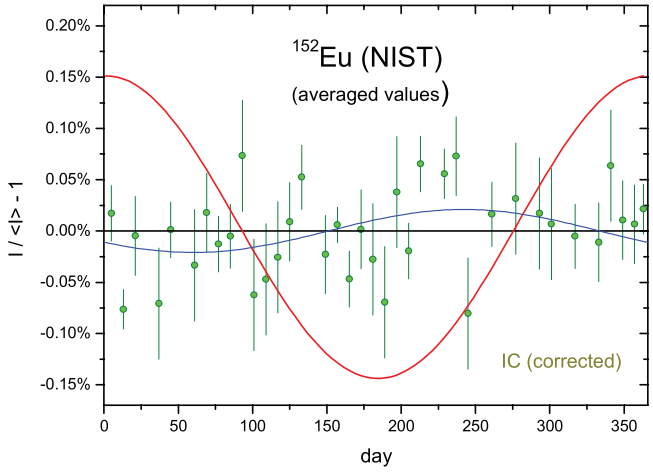

Figure 37. Annual average residuals from exponential decay for ^{152}Eu activity measurements with IC 'A' at NIST.

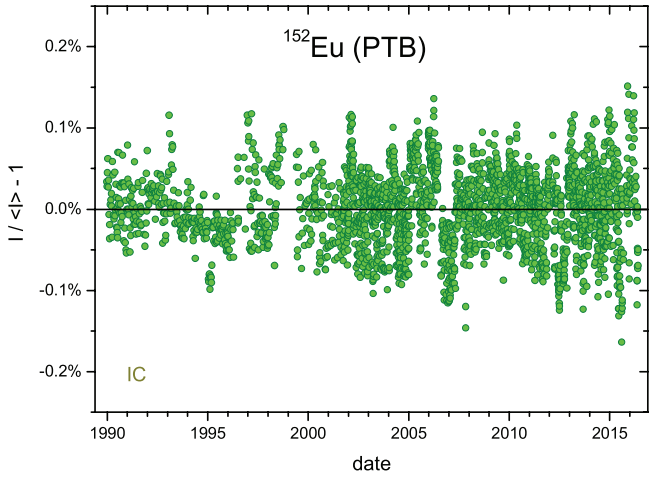

Figure 38. Residuals from exponential decay for ^{152}Eu activity measurements (relative to a ^{226}Ra check source) with the IG12/A20 IC at PTB.

in the 8 HPGe detectors of SCK, as shown in figure 35. This is a very strong indication that the instabilities are of instrumental nature and not caused by 'external' influences.

10.4. ^{152}Eu @NIST

A data set of 96 decay rate measurements obtained between 1976 and 2011 with the IC 'A' [22] of the NIST have been analysed, after applying a linear detrending correction for data obtained after 1986. The residuals in figure 36 are less than 0.15% in amplitude and the annual averages in figure 37 show no explicit seasonality ($A = 0.021\ (9)\%$, $a = 214$ d).

10.5. ^{152}Eu @PTB

At the PTB (Germany), IC measurements of a ^{152}Eu source were repeated 2515 times between 1989 and 2016. The raw ionisation currents obtained before 1999 show 0.1% modulations [10], which can be significantly reduced by analysing the data relative to the ^{226}Ra check source. Most of the resulting residuals are well within 0.1% (figure 38), which leaves little room for potential claims about permille-sized modulations in the ^{152}Eu decay rates at any frequency between a day and several decades. There is a distinct but small annual sinusoidal effect ($A = 0.018\ (1)\%$, $a = 11$ d) in the averaged residuals (figure 39) which appears to be instrument-specific (see e.g. ^{54}Mn in section 3.3, ^{90}Sr, ^{137}Cs in [2] and ^{226}Ra in [1]).

A reanalysis was done of the subset of the raw– i.e. not normalised to the check source—^{152}Eu data published by Schrader [10] in the periods 1990–1995 and 2000–2008. In figures 40 and 41, annual averaged residuals are presented for both periods, after applying linear detrending corrections over 4 time zones in the 2000–2008 data set. The annual modulations ($A = 0.082\ (3)\%$, $a = 63$ d) in the ^{154}Eu data from 1990 to 1995 match those of the ^{226}Ra check source ($A = 0.084\ (5)°\%$, $a = 64$ d) and of ^{154}Eu ($A = 0.081\ (3)\%$, $a = 65$ d) [2] in the same period. The 2000–2008 ^{152}Eu data show a comparably small annual modulation ($A = 0.008\ (3)°\%$, $a = 237$ d), which suggests that the modulations in figure 39 may in part be caused by the normalisation to the ^{226}Ra check source. A similar conclusion was derived from ^{154}Eu β^- decay data in [2].

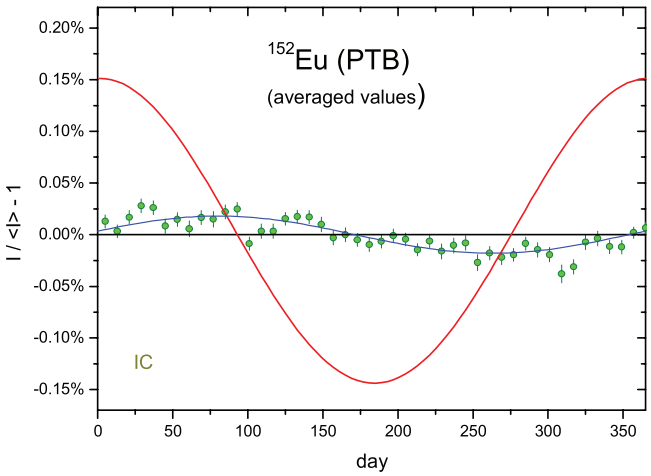

Figure 39. Annual average residuals from exponential decay for ^{152}Eu activity measurements (relative to a ^{226}Ra check source) with the IG12/A20 IC at PTB.

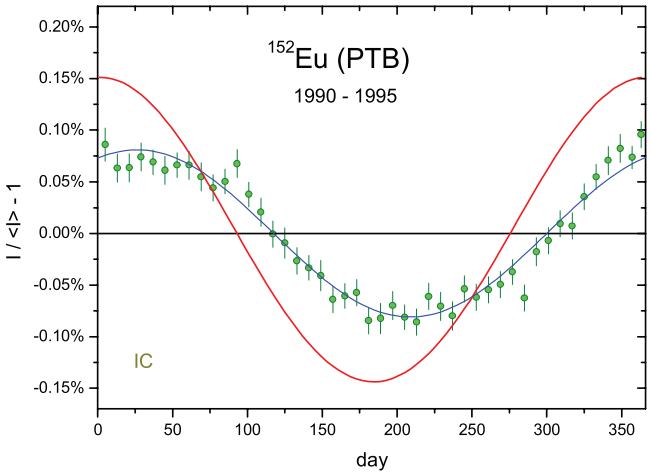

Figure 40. Annual average residuals from exponential decay for ^{152}Eu ionisation current measurements with the IG12/A20 IC at the PTB from 1990 to 1995, using the Townsend balance method for current readout.

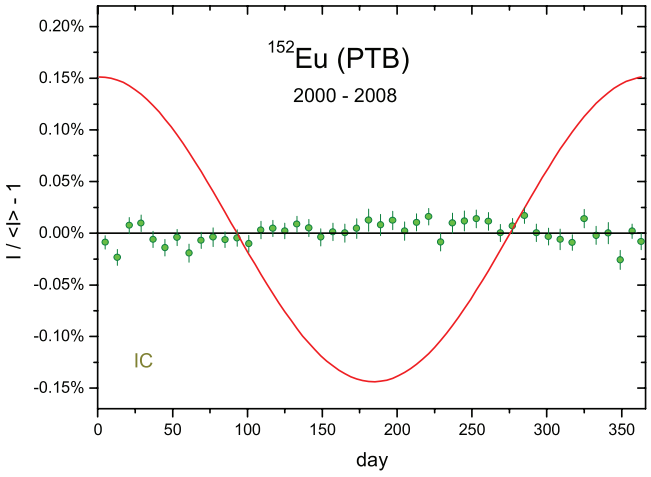

Figure 41. Annual average residuals from exponential decay for ^{152}Eu ionisation current measurements with the IG12/A20 IC at the PTB from 2000 to 2008, using a commercial electrometer for current readout.

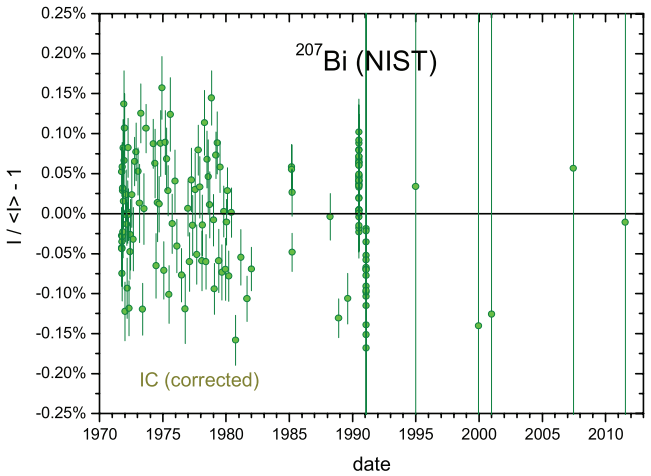

Figure 42. Residuals from exponential decay for ^{207}Bi activity measurements with ionisation chamber 'A' at NIST.

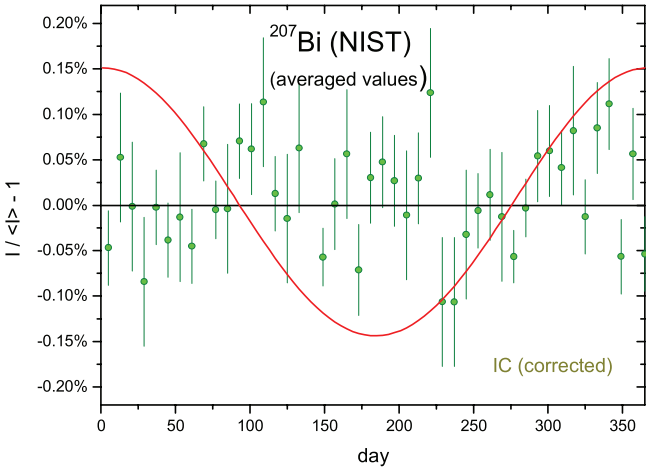

Figure 43. Annual average residuals from exponential decay for ^{207}Bi activity measurements with IC 'A' at NIST.

11. Bismuth-207

11.1. Decay characteristics

Bismuth-207 (32.9 (14) a) decays by EC to exited levels of ^{207}Pb, as well as through a small β^+ branch (0.012%) [21].

11.2. ^{207}Bi @NIST

The decay of a ^{207}Bi source was followed over four decades with the IC 'A' [22] at the NIST. Linear adjustments were made for slow geometrical changes in the source holder [23], and additionally for long-term detrending purposes (over three multi-annual time zones) in this work. The residuals from exponential decay in figure 42 are mostly concentrated in the first decade and in 1990. The annual averaged residuals in figure 43 are mostly within 0.1% and show no appreciable seasonal modulation ($A = 0.004$ (11)%, $a = 23$ d).

12. Conclusions

The decay through β^+ and EC processes shows as little variability with respect to annual oscillations as α or β^- decay. No systematic oscillations in phase with Earth–Sun distance were found. The observed stability of ^{22}Na, ^{54}Mn, ^{65}Zn, ^{82,85}Sr and ^{207}Bi decay rates—within $A = 0.008\%$ or better—is bound by the same instrumental limitations as similar IC measurements for α or β^- emitting nuclides. The experimental evidence is equally convincing for ^{55}Fe ($A = 0.004\%$) in spite of its low-energy radiation and measurement in a gas proportional counter. Good stability was demonstrated for ^{109}Cd ($A = 0.015\%$) and ^{152}Eu ($A = 0.01\%$) measured through IC and γ-ray spectrometry. The data sets presented in parts I–III of this work are typically 50 times more stable than the ones in literature which inspired theories of non-exponential decay. The best experimental evidence confirms the validity of the exponential decay law within the 10^{-5}–10^{-6} level and no proof could be found of violations of the invariability of decay constants.

It has to be recognised that all long-term measurements are vulnerable to instrumental instabilities, which have to be taken into account in the interpretation of observations of auto-correlations in residuals to the exponential decay curve. The measurements with the PTB ionisation chamber, for example, show a small recurrent modulation for several radionuclides which is incompatible with the theory that seasonal changes in the solar neutrino flux changed the decay rate, because it was not reproduced by any of the other laboratories. The fact that non-exponential behaviour in γ-ray spectrometry differs from one spectrometer to another within the same laboratory (see SCK, JSI) strongly suggests that instrumental instability is the root cause rather than a global physical phenomenon.

Owing to the invariability of decay constants, there is no impediment to the establishment of the SI unit becquerel through primary standardisation at 0.1% range accuracy nor to the demonstration of equivalence of activity at the international level over a time span of decades. It is normal for repeated activity measurements to show varying degrees of instability of instrumental and environmental origin and such auto-correlated variability should be taken into account next to statistical variations when setting alarm levels in quality control charts. Taking into account such instabilities and adhering to proper uncertainty propagation, no fundamental objections need to be made against half-life measurement with sub-permille uncertainties, nor against applying exponential decay formulas to calculate activity at a future or past reference time or to perform accurate nuclear dating.

Acknowledgments

The authors thank all past and present colleagues who contributed directly or indirectly to the vast data collection over different periods spanning six decades. They are particularly indebted to Michael Unterweger, Ryan Fitzgerald, Denis Bergeron and Leticia Pibida of the National Institute of Standards and Technology (NIST, USA) for generously providing data sets for various nuclides.

Disclaimer

Certain commercial equipment is identified in this paper to foster understanding. Such identification does not imply recommendation or endorsement by the participating laboratories, nor does it imply that the materials or equipment identified are necessarily the best available for the purpose.

References

[1] Pommé S *et al* 2016 On decay constants and orbital distance to the Sun—part I: alpha decay *Metrologia* **54** 1–18
[2] Pommé S *et al* 2016 On decay constants and orbital distance to the Sun—part II: beta minus decay *Metrologia* **54** 19–35
[3] Pommé S *et al* 2016 Evidence against solar influence on decay constants *Phys. Lett.* B **761** 281–6
[4] Parkhomov A G J 2011 Deviations from beta radioactivity exponential drop *Mod. Phys.* **2** 1310–7
[5] Jenkins J H *et al* 2013 Concerning the time dependence of the decay rate of ^{137}Cs *Appl. Radiat. Isot.* **74** 50–5
[6] Mueterthies M J *et al* 2016 Is there a signal for Lorentz nonvariance in exisiting radioactive decay? arXiv:1607.03541
[7] O'Keefe D *et al* 2013 Spectral content of ^{22}Na/^{44}Ti decay data: implications for a solar influence *Astrophys. Space Sci.* **344** 297–303
[8] Norman E B *et al* 2009 Evidence against correlations between nuclear decay rates and Earth–Sun distance *Astropart. Phys.* **31** 135–7
[9] Nähle O and Kossert K 2015 Comment on 'Comparative study of beta-decay data for eight nuclides measured at the Physikalisch-Technische Bundesanstalt' [*Astropart. Phys.* **59** (2014) 47–58] *Astropart. Phys.* **66** 8–10
[10] Schrader H 2016 Seasonal variations of decay rate measurement data and their interpretation *Appl. Radiat. Isot.* **114** 202–13
[11] Jenkins J H and Fischbach E 2009 Perturbation of nuclear decay rates during the solar flare of 2006 December 13 *Astropart. Phys.* **31** 407–11
[12] Mohsinally T *et al* 2016 Evidence for correlations between fluctuations in ^{54}Mn decay rates and solar storms *Astropart. Phys.* **75** 29–37
[13] Silverman M P 2016 Search for anomalies in the decay of radioactive Mn-54 *Europhys. Lett.* **114** 62001
[14] Van Ammel R *et al* 2010 Measurement of the ^{54}Mn half-life *Appl. Radiat. Isot.* **68** 2387–92
[15] Pommé S 2015 The uncertainty of the half-life *Metrologia* **52** S51–65
[16] Pommé S 2016 When the model doesn't cover reality: examples from radionuclide metrology *Metrologia* **53** S55–64
[17] Lindstrom R 2016 Believable statements of uncertainty and believable science *J. Radioanal. Nucl. Chem.* (doi: 10.1007/s10967-016-4912-4)
[18] Amiot M-N *et al* 2015 Uncertainty evaluation in activity measurements using ionization chambers *Metrologia* **52** S108–22
[19] Lépy M-C, Pearce A and Sima O 2015 Uncertainties in gamma-ray spectrometry *Metrologia* **52** S123–45
[20] Pommé S 2015 The uncertainty of counting at a defined solid angle *Metrologia* **52** S73–85

[21] DDEP, 2004–2013. Table of radionuclides vol 1–7, Monographie BIPM-5 BIPM, Sèvres, website: www.nucleide.org/DDEP_WG/DDEPdata.htm
[22] Unterweger M P and Fitzgerald R 2014 Update of NIST half-life results corrected for ionization chamber source-holder instability *Appl. Radiat. Isot.* **87** 92–4
[23] Fitzgerald R 2012 NIST ionization chamber 'A' sample-height corrections *J. Res. Natl Inst. Stand. Technol.* **117** 80–95
[24] Van Ammel R, Pommé S and Sibbens G 2006 Half-life measurement of ^{55}Fe *Appl. Radiat. Isot.* **64** 1412–6
[25] Van Ammel R *et al* 2004 Experimental verification of the half-life of ^{65}Zn *Appl. Radiat. Isot.* **60** 337–9
[26] Pibida L *et al* 2009 Measurements of the ^{82}Sr half-life *Appl. Radiat. Isot.* **67** 636–40
[27] Fitzgerald R P 2009 An automated ionization chamber for secondary radioactivity standards *Appl. Radiat. Isot.* **68** 1507–9
[28] Van Ammel R *et al* 2011 Measurement of the ^{109}Cd half-life *Appl. Radiat. Isot.* **69** 785–9
[29] Sturrock P A *et al* 2013 An analysis of apparent *r*-mode oscillations in solar activity, the solar diameter, the solar neutrino flux, and nuclear decay rates, with implications concerning the Sun's internal structure and rotation, and neutrino processes *Astropart. Phys.* **42** 62–9
[30] Sturrock P A, Fischbach E, Jenkins J 2014 Analysis of beta-decay rates for Ag^{108}, Ba^{133}, Eu^{152}, Eu^{154}, Kr^{85}, Ra^{226}, and Sr^{90}, measured at the Physikalisch-Technische Bundesanstalt from 1990 to 1996 *Astrophys. J.* **794** 42
[31] Bruggeman M, Verheyen L and Vidmar T 2014 A dedicated LIMS for routine gamma-ray spectrometry *Appl. Radiat. Isot.* **87** 425–8
[32] Pons D J, Pons A D and Pons A J 2015 Hidden variable theory supports variability in decay rates of nuclides *Appl. Phys. Res.* **7** 18–29